# Growth of Thin Film Water on α-$Al_2O_3$ (0001): An FTIR Study

**Alyssa C. Thomas and Hugh H. Richardson***

*Department of Chemistry and Biochemistry, Ohio University, Athens, Ohio 45701*

*Received: August 14, 2008*

This study set out to elucidate the growth of thin film water on a hydroxylated α-$Al_2O_3$ (0001) surface using FTIR spectroscopy. The absorption of water on metal oxide surfaces, particularly aluminum oxides, alters the surface chemical reactivity and structure. We are able to detect an infrared signature due to surface bound water that is different than multilayer water. We use this infrared signature to separate and quantify the amount of water at the surface or interfacial water from the total amount of water adsorbed. Also, we use this information to model the growth of the interfacial water layer as compared to total water absorption and show that initially water does not wet the α-$Al_2O_3$ (0001) surface completely. We are able to extract a small contact angle ($1.9 \times 10^{-4}$) and spreading parameter ($-4 \times 10^{-10}$) for thin-film water growth up to ~7 monolayer equivalents and show that thin-film water grows as droplets that conserve contact angle.



## 1. Introduction

Water interactions at surfaces direct and dictate many important naturally occurring phenomena as well as numerous technological processes.[1−8] Water adsorbs to most surfaces under ambient conditions.[1,7] Surprisingly, the structure, topography and morphology of the initially forming film are still unclear for many surfaces and experimental conditions.[3,9] For example, the adsorption of water on metal oxide surfaces has been extensively studied because these surfaces are naturally ubiquitous and have widely important technological applications.[2−6] But, there is no clear understanding of how water initially adsorbs to these type of surfaces. Water adsorption on metal oxide surfaces is complicated by the fact that the surface is altered when water absorbs. The hydroxylation/dehydroxylation of α-$Al_2O_3$ surfaces are believed to have a common mechanism[10−16] while water adsorption on a hydrated surface will be markedly different than adsorption on a nonhydrated one.

In this paper, we study the adsorption of water on an ultrasmooth hydroxylated α-$Al_2O_3$ (0001) surface that has been treated so that water readily adsorbs to it. We have investigated the structure and morphology of the initially forming film with attenuated partial internal refection (APR) infrared spectroscopy. We are able to detect an infrared signature due to interfacial water that is different than multilayer water and show that water does not fully wet the surface even when the amount of water adsorbed on the surface is equivalent to 7 monolayers. We measured a contact angle ($1.9 \times 10^{-4}$) and spreading parameter ($-4 \times 10^{-10}$) that is invariant with the amount of water adsorbed on the surface. Our results show that the growth of the initial water film is dictated by the interfacial tensions between the three phases (solid/liquid/gas) and that incomplete wetting with growth of water droplets with constant contact angle ($1.9 \times 10^{-4}$) is observed.

## 2. Experiment

A custom-made triangular 45° × 45° × 90° α-$Al_2O_3$ prism (Reflex Analytical Corporation) was used with (0001) oriented and polished sides. The prism was annealed in a sapphire crucible at 1450 °C for 24 h under ambient conditions to produce an ultrasmooth surface.[17] Prior to use, it was cleaned in a dilute piranha solution for 20 min to rid the surface of organic matter. It was then rinsed thoroughly with 18 MΩ water to completely hydroxylate the surface[18] and dried with a stream of $N_2$ gas. It was immediately inserted into the experimental sample chamber (Figure 1) and stored under vacuum ($10^{-3}$ Torr). Based on previous applications,[19,20] a modified FastIR (Harrick Scientific) serves as a sample chamber for thin film water experiments. The largest square face of the prism fits flush into the copper plate which serves to seal the sample chamber. Mounted mirrors inside the assembly allow it to be used in the sample compartment of a typical FTIR. An alumel−chromel (K type) thermocouple attached to a nonpolished triangle face of the prism using thermal tape is used to check and equilibriate the temperature. Attached to the copper plate on either side of prism are two thermoelectric peltier coolers (Melcor) allowing for manipulation of the prism's temperature through the use of a power supply. The prism surface was isolated from the surroundings by a stainless steel cap connected to a vacuum pump assembly. The cap screws into the copper plate and an O-ring provides a direct seal to the prism surface. Attached to the same pump assembly is a reservoir containing 18 MΩ water that has been degassed by several freeze/thaw cycles. The temperature of the water is

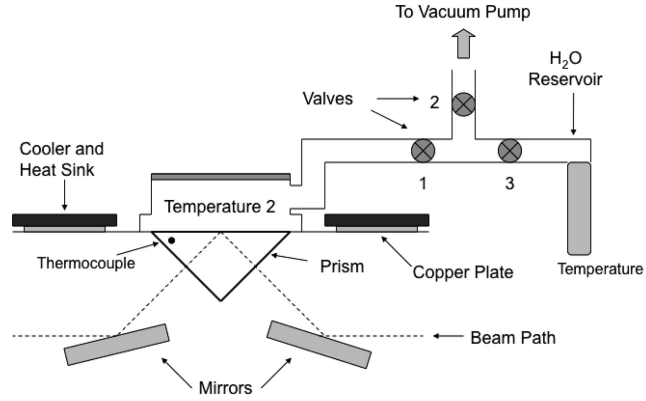


**Figure 1.** Schematic representation of the experimental setup used to collect extinction spectra using attenuated partial internal reflection (APR) IR spectroscopy for $H_2O$ adsorbed on α-$Al_2O_3$.

* To whom correspondence should be addressed. E-mail: richards@helios.phy.ohiou.edu.

10.1021/jp8072766 CCC: $40.75 
Published on Web 11/21/2008

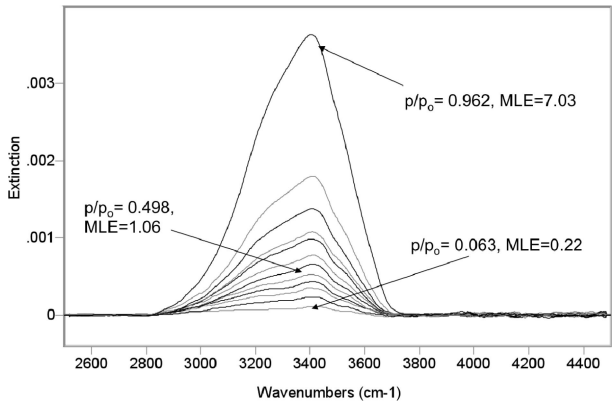


**Figure 2.** Representative extinction spectra of the O−H stretching region are shown for $H_2O$ adsorbed on α-$Al_2O_3$ (0001) at 15 °C. The bands are broad and asymmetric with shoulders at ∼3200 and ∼3500 $cm^{-1}$. The band shapes and centers for 15, 17, and 19 °C at comparable MLE are almost identical.

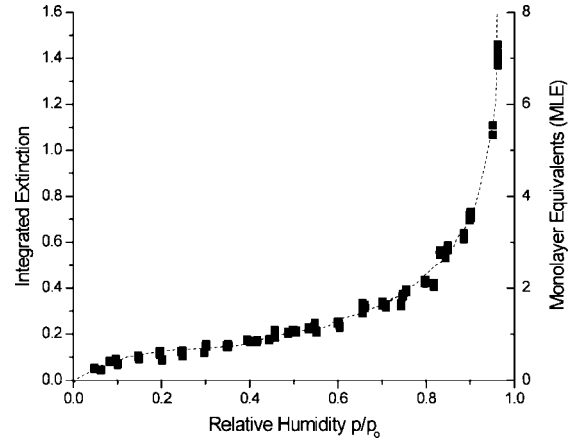


**Figure 3.** $H_2O$ adsorption/desorption isotherms for 15, 17, and 19 °C plotted as a function of relative humidity, integrated extinction and monolayer equivalents. The isotherms are nearly superimposable, are smooth, and showed little or no hysteresis during data collection.

controlled by a circulating water bath of known temperature checked by another K type thermocouple. The prism and water reservoir are separated by three valves in the vacuum pump assembly, which when manipulated allow for data collection. All parts of the vacuum pump assembly are made of stainless-steel.

To begin data collection, the prism (Temperature 1) and the water reservoir (Temperature 2) and are allowed to equilibrate to the desired temperature for 1 h. Valves 1 and 2 are open and a background spectrum is collected under vacuum. The sample chamber and spectrometer compartment are purged with dry $N_2$ gas to eliminate excess water vapor in the spectrum. Upon its completion, Valve 2 is closed and Valve 3 opened to allow water vapor from the reservoir to travel to the prism surface. To avoid unwanted condensation in the vacuum lines or stainless steel cap, the whole assembly is wrapped in heat tape. The water vapor is allowed to equilibrate for one minute before the experimental spectrum is collected. Additional equilibrium time showed no significant differences in resulting spectra. Fourier-transform infrared (FTIR) transmission spectra are collected using a Bruker IFS 66 spectrometer equipped with an Indium-Antimonide (InSb) detector. Spectra collected consisted of 512 double-sided interferograms coadded, and Fourier-transformed to produce a spectrum with 4 $cm^{-1}$ resolution. A ratio of the experimental spectrum with its corresponding background spectrum yields an extinction spectrum for each temperature measurement. The resultant spectra are truncated (2500 $cm^{-1}$ to 4500 $cm^{-1}$) to isolate the O−H stretching region and baseline corrected using Grams/AI software (Galatic Industries).

## 3. Results

**3.1. Extinction Spectra of Water on α-$Al_2O_3$ (0001).** Representative extinction spectra for $H_2O$ adsorbed on α-$Al_2O_3$ (0001) at 15 °C are shown in Figure 2. Data was collected as a function of water vapor pressure or relative humidity (RH). The RH values are defined as $p/p_o$, where $p$ is the water vapor pressure over the substrate and $p_o$ is its equilibrium value over water at the designated temperature. The pressures are determined by the corresponding temperature of the water reservoir and prism, respectively. We will quantitatively relate the integrated extinction, $\tilde{E}$, to an amount of water adsorbed in monolayer equivalents (MLE) in the Discussion.

The bands are broad with a full width at half-height (fwhh) of ∼400 $cm^{-1}$. The band shape is asymmetric with a shoulder at ∼3200 $cm^{-1}$. Another shoulder at ∼3500 $cm^{-1}$ is easily observed at MLE less than ∼7. Unlike previous FTIR studies of metal oxides such as $Al_2O_3$[21] and MgO,[22,23] the spectra do not exhibit a negative peak between 3600−3700 $cm^{-1}$. The overall band shape and features are conserved at lower MLE. The O−H stretching region for the adsorbed water closely resembles that of bulk water.[20,24,25] Further discussion will follow on the difference in band shape between the adsorbed and bulk water.

Spectra taken sequentially for increasing pressure are nearly superimposable for spectra taken with decreasing pressure. The spectra show little or no hysteresis. The band shapes and band centers for all three temperatures explored (15, 17, and 19 °C) at comparable MLE are almost identical. The numerous spectra collected under these experimental circumstances were done so over a few months' time with excellent reproducibility.

**3.2. Adsorption and Desorption Isotherms.** The water adsorption and desorption isotherms at 15, 17, and 19 °C are shown in Figure 3. The integrated extinction area for the water band is plotted against relative humidity. The amount of water on the surface in MLE is determined using the method described in section 4.1. The adsorption and desorption isotherms for each temperature showed little or no hysteresis. Also, the isotherms are nearly superimposable for the different temperatures probed. The thermodynamic parameters for the heat and entropy of adsorption are the same as bulk liquid values within the uncertainty of our measurement. The uncertainty can be reduced by examining a larger temperature range and subtle differences between the thin film water and bulk liquid might be detected. Unfortunately, these type of measurements average over the entire water population and are inherently insensitive to interfacial adsorption for monolayer equivalences greater than one.

## 4. Discussion

**4.1. The Amount of Water Adsorbed in MLE.** The extinction measurements can be quantified in terms of water adlayer monolayer equivalents (MLE). The spectroscopic signatures of bulk water and thin film water on α-$Al_2O_3$ are very similar suggesting that the hydrogen bonding environments are similar and the optical constants should be nearly identical. We use the integrated extinction, $\tilde{E}$, of the thin water film spectrum to determine the amount of water, in MLE, on the surface by knowing the integrated cross section, $\bar{\sigma}$, of bulk water ($1.4 \times 10^{-16}$ cm/molecule[26]) and applying eqs 1 and 2. In these

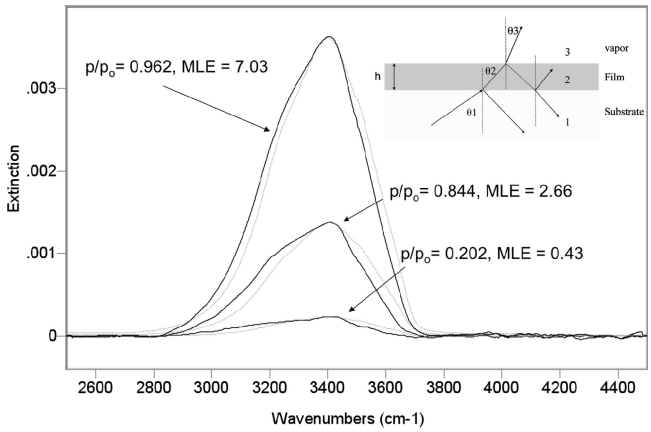


**Figure 4.** Experimental spectra (solid dark lines) for the water adlayer are compared with thin film water reference spectra (lighter lines) calculated using bulk water optical constants. Inset: The thin film water was modeled as a uniformly thick layer with height $h$ sandwiched between $\alpha$-$Al_2O_3$ and the surrounding vapor.

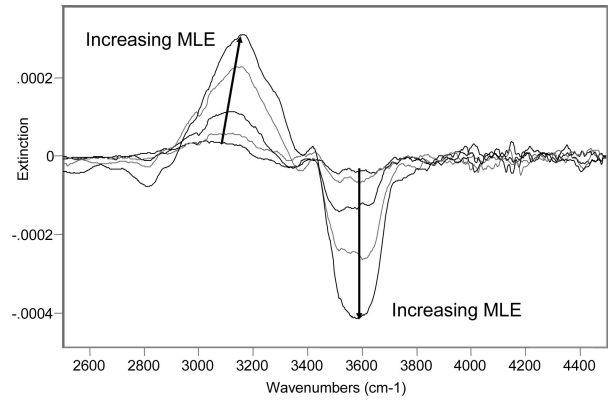


**Figure 5.** Shown are the representative difference spectra for the comparison of experimental water adlayer to a reference thin film of water. The spectra show two prominent features: (1) a positive band at ~3000 $cm^{-1}$ assigned to $H_2O$ adsorbed on the surface (interfacial water) and (2) a negative band at 3550 $cm^{-1}$ assigned to $H_2O$ molecules with limited or no connectivity to other $H_2O$ molecules.

equations $S_{H_2O}$ is the surface density (molecules/$cm^2$) and $S_{H_2O,\theta=1}$ is the monolayer equivalence of water molecules corresponding to a single monolayer.

$$\tilde{E} = \frac{S_{H_2O}\bar{\sigma}\alpha}{2.303} \quad (1)$$

$$\mathrm{MLE} = \frac{S_{H_2O}}{S_{H_2O,\theta=1}} \quad (2)$$

In eq 1, the $\tilde{E}$ comes from spectra collected using APR which has a higher sensitivity than attenuated total internal reflection (ATR) spectroscopy and transmission.[20] In order to determine the sensitivity of our APR experiment, we used the bulk optical constants of liquid water to calculate the expected spectra for a single uniform monolayer of water[20,24,25] (see inset in Figure 4) in terms of extinction and absorbance. For our APR experiment, the incident angle, $\theta_1$, is set to 45° resulting in an extinction of $5.3 \times 10^{-4}$ at 3400 $cm^{-1}$ for a single monolayer. In a transmission experiment, $\theta_1$ is set as 0° resulting in an absorbance of $1.6 \times 10^{-4}$ at 3400 $cm^{-1}$. The response of APR under these experimental conditions is greater than transmission by a factor of 3.25, denoted as $\alpha$ in eq 1.

The monolayer equivalence, $S_{H_2O,\theta=1}$, is the surface density of liquid water ($1.04 \times 10^{15}$ molecules/$cm^2$). The surface density of liquid water is used as the monolayer equivalence because the extinction spectra for the thin-film water are nearly superimposable upon the calculated spectra using liquid water optical constants. There is a discrepancy between the surface layer and liquid water but the subsequent layers are liquid-like (see section 4.3, Spectroscopic Analysis of Water Adsorption). In our analysis, we assume that all layers have the surface density of liquid water.

**4.2. Isotherm Characteristics.** The shape of the isotherm reveals interactions, such as hydrogen bonding environments[27] and wetting characteristics,[28] between the adsorbing species and the surface. Changes in the isotherm shape, or lack thereof, can show how these interactions change with temperature and pressure. The shape of the isotherm, shown in Figure 3, is characteristic of a Brunauer's type III isotherm[29,30] where adsorption asymptotically approaches $p/p_o = 1$. At low pressure values, the adlayer amount is also low suggesting a weak affinity between water vapor and the $\alpha$-$Al_2O_3$ surface. There are no abrupt changes in the isotherm shape as $p/p_o$ increases and the smoothness indicates that there are no phase transitions within the film in this temperature range.[28] The smoothness of the isotherm also provides evidence that the hydrogen bonding environments of the adsorbed water are not distinctly layered and if changes in these environments due to pressure occur, they happen in a gradual manner.[27]

**4.3. Spectroscopic analysis of water adsorption.** A spectroscopic analysis of the O−H stretching region was initiated to obtain structural information about the water adlayer. Extinction spectra from a thin water film (modeled as a thin film with uniform thickness between two infinitely thick media, substrate and vapor) was calculated using the bulk optical constants of liquid water[20,24,25] (see inset in Figure 4). This water slab will be referred to as the reference film. Figure 4 compares the extinction spectra for the water adlayer to the spectra of the reference film. The substrate temperature is 15 °C and water amounts of 0.43, 2.66 and 7.03 MLE are presented. The solid darker lines are the measured spectra for the water adlayer while the lighter lines are the reference spectra. Notice that the reference spectra under represents the adlayer spectra at the low wavenumber side of the band and over represent the adlayer spectra on the high wavenumber side of the band. A difference spectrum (experimental minus calculated) was obtained by matching the integrated extinction of the adlayer spectra with the reference spectra and then carrying out the subtraction. This analysis highlights the deviation between the adlayer spectra and the reference spectra. A positive extinction in the difference spectra uncovers water molecules in the water adlayer that are not as abundant in the reference film while a negative difference reveals water molecules that are more abundant in the reference film. The reference film in this case is liquid water that completely covers the surface and has a uniform thickness.

A plot of the difference spectra for increasing MLE is shown in Figure 5. Two major features are evident. The first is a positive peak, shifted to lower wavenumbers relative to bulk water, whose integrated extinction increases with increasing MLE. The second feature is a negative peak centered at 3550 $cm^{-1}$ whose integrated extinction also increases with increasing MLE. The positive peak maximum shifts toward higher values with increasing MLE. The wavenumber at peak maximum ($\bar{\nu}_{max}$) is centered at 3026 $cm^{-1}$ for a MLE of 0.43 and shifts to 3164 $cm^{-1}$ at a MLE of 7.03. Figure 6 highlights these spectra shifts where $\bar{\nu}_{max}$ is plotted for all three substrate temperatures acquired at different MLE. We assign this peak to water molecules bound

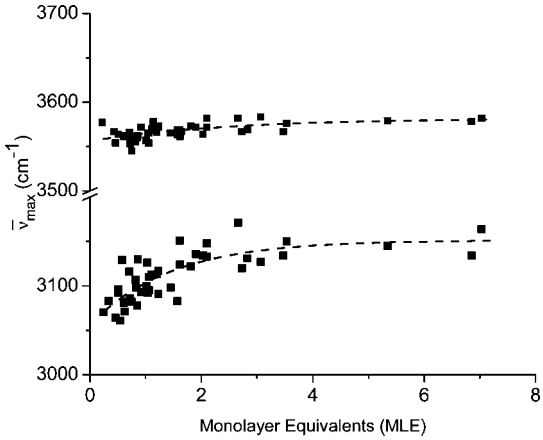


**Figure 6.** Peak maximum, $\bar{\nu}_{max}$, for the positive (lower) and negative (upper) peaks of the difference spectra in Figure 5 are plotted as a function of MLE at 15, 17, and 19 °C. The positive $\bar{\nu}_{max}$ shifts from 3026 to 3164 $cm^{-1}$ as the MLE increase, while the negative $\bar{\nu}_{max}$ centered at 3550 $cm^{-1}$ is invariant to changes in MLE.

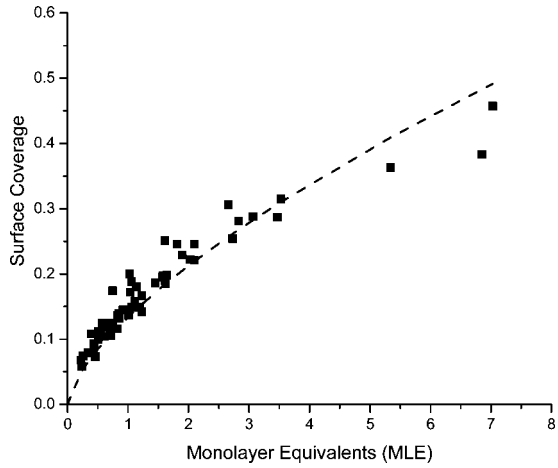


**Figure 7.** Amount of interfacial water is plotted against the total amount of $H_2O$ adsorbed at 15, 17, and 19 °C. Initially, the surface coverage linearly increases with MLE which suggests partial wetting and a preference for 3D island growth. At ~7 MLE, only 55% of the α-$Al_2O_3$ surface is covered.

at the surface (interfacial water). Water molecules in stronger hydrogen bonding environment than liquid water have lowered O−H stretching frequencies[31] relative to the liquid and this assignment is consistent with water molecules that are bound at the solid/liquid interface. The negative peak maximum centered at 3550 $cm^{-1}$ does not shift with increasing MLE. We assign this band to water molecules that are have limited connectivity to other water molecules. The negative band reveals water molecules that have a greater amount in the reference (liquid water) than in the sample (interfacial water). Our results show that interfacial water has less nonconnected water molecules than liquid water.

The integrated extinction for the interfacial water band can be used to determine the amount of water adsorbed on the surface. This procedure assumes that there is not a significant deviation in the optical cross section of water in the interfacial region compared to liquid water. Figure 7 plots the amount of water found at the interfacial region in coverage units to the total amount of water adsorbed for all three temperatures. No significant temperature dependence is observed for the coverage of interfacial water compared to the total MLE of water on the substrate. The most striking feature of Figure 7 is that a portion of the surface is not covered with water (55%) even though

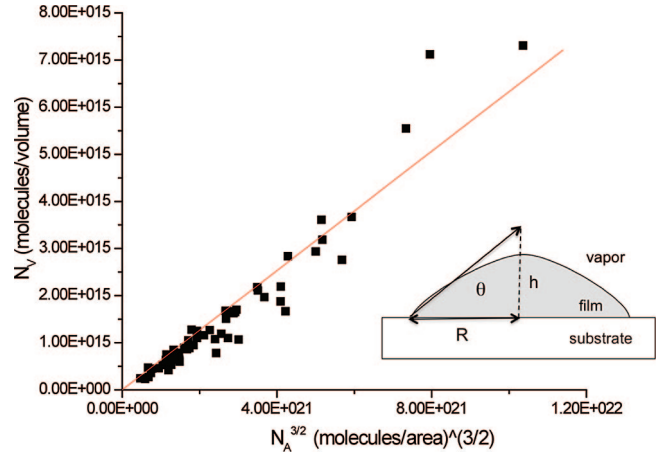


**Figure 8.** The plot of total $H_2O$ molecules in a droplet, $N_v$, versus the $H_2O$ molecules adsorbed on the surface, $N_A^{3/2}$, shows a linear trend with a slope of $6.0 \times 10^{-7}$. A contact angle ($1.9 \times 10^{-1}$) and spreading parameter ($-4 \times 10^{-10}$) are determined from the slope. Inset: A cone with radius $R$ and height $h$ is used to approximate the volume of a water droplet with contact angle $\theta$.

many monolayer equivalents of water (~7) have been adsorbed on the surface. The initial stage of water growth shows a preference for three-dimensional island growth instead of completely wetting the surface. How can we understand why water, at least in the initial stage of growth, prefers island growth instead of layer by layer growth?

**4.4. Model of Water Adsorption.** Our model assumes that water grows on the surface characteristic of incomplete wetting with droplets that have a nonzero contact angle. The number of molecules on the $Al_2O_3$ surface (molecules/area) can be determined using the interfacial coverage assuming a surface concentration of $\sim 10^{15}$ molecules/$cm^2$, while the total number of molecules in the water droplet (molecules/volume) can be determined using the total monolayer equivalents. The volume of a water droplet is approximated as a cone of radius $R$ and height $h$ (see inset in figure 8). The volume is then $V = (\pi R^2 h)/3$ and the area on the surface is $A = \pi R^2$. The contact angle is obtained using $\tan\theta = (h)/R$. Solving for $R$ in terms of $A$ and $\theta$ gives the volume as $V = (A^{3/2} \tan\theta)/3\sqrt{\pi}$. The water volume and area scales with the number of molecules so that $N_V = (N_A^{3/2}\tan\theta)/3\sqrt{\pi}$ where $N_V$ is the number of molecules in the water volume and $N_A$ is the number of molecules on the surface. If our model is correct then a plot of $N_V$ against $N_A^{3/2}$ should give a straight line with a slope of $(\tan\theta)/3\sqrt{\pi}$. The contact angle can be determined from the slope. Figure 8 shows such a plot and the linear trend as expected. The slope is $6.0 \times 10^{-7}$ yielding a contact angle of $1.9 \times 10^{-4}$. From the contact angle a spreading parameter of $-4 \times 10^{-10}$ is obtained using $S = \gamma(\cos\theta - 1)$where $\gamma$ (73 mN/m) is the surface tension of water.[32] Figure 8 shows that water grows on the $Al_2O_3$ surface as droplets that conserve contact angle.

## 5. Conclusions

We were able to elucidate the structure of water absorbed on a hydroxylated α-$Al_2O_3$ (0001) surface using FTIR spectroscopy. Water adsorption and desorption isotherms were collected at 15, 17, and 19 °C and showed little or no hysteresis with nearly superimposable shape. The isotherm shape is smooth with low MLE adsorbed at low pressure values, indicating a weak affinity between the water vapor and the α-$Al_2O_3$ surface. The smoothness and lack of abrupt changes in the isotherm shape are

evidence that the hydrogen bonding environment is not distinctly layered and if changes occur, they are gradual over the pressure range.

Further spectroscopic analysis of the O−H stretching region provides additional information on the surface adlayer structure. The observed spectral differences between the adsorbed film and a reference film for liquid water reveals a positive band centered at ~3100 $cm^{-1}$ and a negative band at ~3550 $cm^{-1}$. The positive difference band is assigned to water molecules hydrogen bonded to surface hydroxylated groups or interfacial water. The negative band is assigned to non-networked water more abundant in liquid water than in thin-film water. We extracted the amount of interfacial water and compared it to the total adsorbed water and found that a significant portion of the surface (55%) is not covered with water even though a total of ~7 MLE is adsorbed. This suggests that water incompletely wets the surface and grows as droplets on the surface. We show that the initial growth of water is dictated by the interfacial tensions between the solid, liquid and gas phases and that incomplete wetting occurs with growth of water droplets at constant contact angle ($1.9 \times 10^{-4}$).

**Acknowledgment.** The authors thank George Ewing for his helpful discussions and guidance with this project. The authors also thank Bascom French for his assistance with design and construction of experimental elements. Funding for this project was provided by Ohio University through a Research Challenge Grant and the Condensed Matter and Surface Science Program.

## References and Notes

(1) Ewing, G. E. Ambient thin film water on insulator surfaces. *Chem. Rev.* **2006**, *106*, 1511–1526.

(2) Jayaraman, K.; Okamoto, K.; Son, S. J.; Luckett, C.; Gopalani, A. H.; Lee, S. B.; English, D. S. Observing capillarity in hydrophobic silica nanotubes. *J. Am. Chem. Soc.* **2005**, *127*, 17385–17392.

(3) Verdaguer, A.; Sacha, G. M.; Bluhm, H.; Salmeron, M. Molecular structure of water at interfaces: Wetting at the nanometer scale. *Chem. Rev.* **2006**, *106*, 1478–1510.

(4) Jai, C.; Aime, J. P.; Mariolle, D.; Boisgard, R.; Bertin, F. Wetting an oscillating nanoneedle to image an air-liquid interface at the nanometer scale: Dynamical behavior of a nanomeniscus. *Nano Lett.* **2006**, *6*, 2554–2560.

(5) Soolaman, D. M.; Yu, H. Z. Water microdroplets on molecularly tailored surfaces: Correlation between wetting hysteresis and evaporation mode switching. *J. Phys. Chem. B* **2005**, *109*, 17967–17973.

(6) Lee, W.; Jin, M. K.; Yoo, W. C.; Lee, J. K. Nanostructuring of a polymeric substrate with well-defined nanometer-scale topography and tailored surface wettability. *Langmuir* **2004**, *20*, 7665–7669.

(7) Ewing, G. E. Thin film water. *J. Phys. Chem. B* **2004**, *108*, 15953–15961.

(8) Shen, Y. R.; Ostroverkhov, V. Sum-frequency vibrational spectroscopy on water interfaces: Polar orientation of water molecules at interfaces. *Chem. Rev.* **2006**, *106*, 1140–1154.

(9) Xu, C.; Goodman, D. W. Structure and geometry of water adsorbed on the MgO(100) surface. *Chem. Phys. Lett.* **1997**, *265* (3−5), 341–346.

(10) Fu, Q.; Wagner, T.; Ruhle, M. Hydroxylated alpha-Al2O3 (0001) surfaces and metal/alpha-Al2O3 (0001) interfaces. *Surf. Sci.* **2006**, *600*, 4870–4877.

(11) Qin, F.; Magtoto, N. P.; Kelber, J. A. Moisture-induced instability at the Al2O3/Ni3Al(110) interface: interfacial chemistry. *Mater. High Temp* **2004**, *21* (4), 193–204.

(12) Mui, C.; Senosiain, J. P.; Musgrave, C. B. Initial oxidation and hydroxylation of the Ge(100)-2 × 1 surface by water and hydrogen peroxide. *Langmuir* **2004**, *20*, 7604–7609.

(13) Garza, M.; Magtoto, N. P.; Kelber, J. A. Characterization of oxidized Ni3Al(110) and interaction of the oxide film with water vapor. *Surf. Sci.* **2002**, *519*, 259–268.

(14) Liu, P.; Kendelewicz, T.; Brown, G. E.; Nelson, E. J.; Chambers, S. A. Reaction of water vapor with alpha-Al2O3(0001) and alpha-Fe2O3(0001) surfaces: synchrotron X-ray photoemission studies and thermodynamic calculations. *Surf. Sci.* **1998**, *417*, 53–65.

(15) Yang, X. F.; Sun, Z. X.; Wang, D. S.; Forsling, W. Surface acid-base properties and hydration/dehydration mechanisms of aluminum (hydr)oxides. *J. Colloid Interface Sci.* **2007**, *308*, 395–404.

(16) Hass, K. C.; Schneider, W. F.; Curioni, A.; Andreoni, W. The chemistry of water on alumina surfaces: Reaction dynamics from first principles. *Science* **1998**, *282* (5387), 265–268.

(17) Yoshimoto, M.; Maeda, T.; Ohnishi, T.; Koinuma, H.; Ishiyama, O.; Shinohara, M.; Kubo, M.; Miura, R.; Miyamoto, A. Atomic-Scale Formation of Ultrasmooth Surfaces on Sapphire Substrates for High-Quality Thin-Film Fabrication. *Appl. Phys. Lett.* **1995**, *67*, 2615–2617.

(18) Eng, P. J.; Trainor, T. P.; Brown, G. E.; Waychunas, G. A.; Newville, M.; Sutton, S. R.; Rivers, M. L. Structure of the hydrated alpha-Al2O3 (0001) surface. *Science* **2000**, *288* (5468), 1029–1033.

(19) Harrick, N. J. Prism Liquid Cell. *Appl. Spectrosc.* **1983**, *37*, 573–575.

(20) Zhang, Z. F.; Ewing, G. E. Attenuated partial internal reflection infrared spectroscopy. *Anal. Chem.* **2002**, *74*, 2578–2583.

(21) Al-Abadleh, H. A.; Grassian, V. H. FT-IR study of water adsorption on aluminum oxide surfaces. *Langmuir* **2003**, *19*, 341–347.

(22) Foster, M.; D'Agostino, M.; Passno, D. Water on MgO(100) - An infrared study at ambient temperatures. *Surf. Sci.* **2005**, *590*, 31–41.

(23) Foster, M.; Furse, M.; Passno, D. An FTIR study of water thin films on magnesium oxide. *Surf. Sci.* **2002**, *502*, 102–108.

(24) Sadtchenko, V.; Ewing, G. E.; Nutt, D. R.; Stone, A. J. Instability of ice films. *Langmuir* **2002**, *18*, 4632–4636.

(25) Cantrell, W.; Ewing, G. E. Attenuated (but not Total) Internal Reflection FT-IR Spectroscopy of Thin Films. *Appl. Spectrosc.* **2002**, *56*, 665–669.

(26) Foster, M. C.; Ewing, G. E. Adsorption of water on the NaCl(001) surface. II. An infrared study at ambient temperatures. *J. Chem. Phys.* **2000**, *112*, 6817–6826.

(27) Cantrell, W.; Ewing, G. E. Thin film water on muscovite mica. *Journal of Physical Chemistry B* **2001**, *105* (23), 5434–5439.

(28) Dash, J. G. Clustering and percolation transitions in helium and other thin films. *Phys. Rev. B* **1977**, *15* (6), 3136–3146.

(29) Adamson, A. W. *Physical Chemistry of Surfaces*, 5th ed.; Wiley & Sons: New York, 1990.

(30) Barnes, G. T.; Gentle, I. R., *Interfacial Science*. Oxford University Press: Oxford, 2005.

(31) Badger, R. M.; Bauer, S. H. Spectroscopic Studies of the Hydrogen Bond. II. The Shift of the O-H Vibrational Frequency in the Formation of the Hydrogen Bond. *J. Chem. Phys.* **1937**, *5*, 839–851.

(32) de Gennes, P.-G.; Brochard-Wyart, F.; Quere, D., *Capillarity and Wetting Phenomena Drops, Bubbles, Pearls, Waves*; Springer-Verlag: New York, 2004.

JP8072766